DOI: 10.1002/ejic.201100443

Mechanistic Insights on the Ruthenium-Catalyzed Hydrogenation of Amides – C–N vs. C–O Cleavage

David Cantillo*[a]

Keywords: Hydrogenation / Metal catalysis / Ruthenium / Pincer complexes / Density functional calculations

Ruthenium-catalyzed amide hydrogenation was thoroughly explored by means of DFT calculations. All the plausible pathways, including those involving the amide or imine tautomer, were assessed. The classical C–O cleavage and the recently reported C–N cleavage were compared by employing a bipyridyl-based Ru^{II} pincer complex as catalyst in the calculations. The study reveals that C–O cleavage can be achieved directly over the amide substrate or its imine tautomer, since the computed pathways show analogous energy barriers. In addition, the mechanism for the novel C–N cleavage was elucidated by modeling all the reasonable intermediates and transition structures. The computed energy barrier is lower than that for C–O cleavage by more than 10 kcal mol^{-1}, thus explaining the observed selectivity. The key role of the aromatization/dearomatization processes during the transformation is also disclosed.

Introduction

Catalytic hydrogenation is one of the most important and versatile reactions in organic synthesis. A broad range of substrates can be reduced by this method, and the design of efficient catalysts is still a challenge for organic chemists.[1]

Reduction of carboxylic acid derivatives such as amides is a very difficult process.[1] It generally requires hydride reagents, which lead to high amount of waste,[2] or drastic conditions (the copper chromite system, for instance, requires temperatures of 250 °C and 300 atm hydrogen pressure).[3] The reported amide hydrogenations with H_2 promoted by Mo/Rh,[4] Re/Rh,[5] or Ru[6] catalysts involve the C–O bond cleavage, which afford secondary amines with water as side product.

Recently, Milstein and co-workers have reported the hydrogenation of amides with cleavage of the alternative C–N bond,[7] employing relatively mild conditions and a dearomatized, bipyridyl-based Ru^{II} pincer complex. This unexpected and unprecedented transformation leads to the amine and the alcohol, and would take place through metal–ligand cooperation (Scheme 1).[7] Since Ru^{II}-catalyzed amide hydrogenations described so far involve cleavage of the C–O bond, the novel complexes, and particularly the possibility of aromatization/dearomatization of the ligand, must play a leading role in the catalytic hydrogenation.

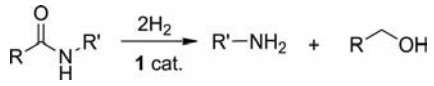

Scheme 1. Hydrogenation of amides by cleaving the C–N bond.

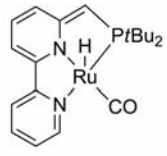

1

Ruthenium-catalyzed hydrogenations of diverse substrates have been previously studied by means of DFT calculations. These studies include the reduction of aldehydes,[8] ketones,[9] and imines.[10] Ruthenium-catalyzed dehydrogenation of ammonium boranes has also been analyzed through DFT calculations.[11] However, to the best of our knowledge, the Ru^{II}-assisted hydrogenation of amides has not yet been computationally addressed.

Herein we report an in-depth mechanistic analysis of the hydrogenation of amides assisted by ruthenium-based catalysts. The expected C–O cleavage[4–6] was compared with the novel C–N cleavage mentioned above.[7] In order to properly compare the energetics involved in both pathways, PNN Ru^{II} pincer catalyst **1** was systematically employed in our calculations.

Computational Details

All the calculations reported in this work were carried out by using the Gaussian09 package.[12] The M06[13] density functional method was selected for all the geometry optimizations and frequency analyses. This DFT approach

[a] Departamento de Química Orgánica e Inorgánica, Universidad de Extremadura
Avda. de Elvas s/n, 06071 Badajoz, Spain
E-mail: dcannie@unex.es

Supporting information for this article is available on the WWW under http://dx.doi.org/10.1002/ejic.201100443.

has been recently recommended for theoretical calculations involving organometallic compounds.[14] The geometry optimizations were performed by using the 6-311G(d,p) basis set for C, H, N, O, and P atoms, while the Stuttgart-Dresden (SDD) basis set,[15] augmented with an f-polarization function,[16] was used to model the Ru atom. All the geometries were optimized including the solvation effects. For this purpose the SMD[17] solvation method was employed, with tetrahydrofuran (THF) as solvent. Frequency calculations as well as geometry optimizations were carried out at the same level of theory to ascertain the nature of the stationary points. Ground and transition states were characterized by zero and one imaginary frequencies, respectively. The electronic energies were improved by single-point calculations by using the 6-311+G(d,p) basis set for the nonmetal atoms. *N*-Ethylacetamide (**4**) was selected as model substrate, because it is one of the amides experimentally employed[7] and exhibits adequate simplicity for theoretical calculations. All the relative energies given are free energies with respect to the reactants (**1** + **4** + $2H_2$), calculated at 298 K and 1 atm. Thermodynamic analyses for reactants and key transition structures were also performed at 383 K and 10 atm to reproduce the experimental conditions[7] and assure that this change does not modify the conclusions drawn. When chiral centers were formed during the transition states, all the possible stereoisomeric structures were computed. The free energies shown in this paper refer to the most stable isomer. Full details are presented in the Supporting Information.

Results and Discussion

In principle, the hydrogenation of the amide group could take place both directly over the substrate and the imine tautomer.[4] The calculated free energies favor the amide species by 16.3 kcal mol^{-1}. This relatively high energy difference would shift the tautomeric equilibrium to the amide form and make the involvement of the tautomer unlikely. However, the high nucleophilicity of the imine could also stabilize pre-reaction complexes with ruthenium, and accordingly the hydrogenation pathway involving this compound has been taken into account as well.

The proposed catalytic cycle for amide hydrogenation starts with the aromatization of pincer complex **1** (Figure 1, Pathways A and A′). In this process, **1** reacts with H_2 to yield ruthenium dihydride **3**. Firstly, H_2 would interact with **1** to give rise to complex **2**. The approach of the hydrogen molecule to the ruthenium atom is a barrierless process, though endergonic by +7.6 kcal mol^{-1} due to the entropy effect. The overall process for the conversion of **1** to **3** is favorable by –1.7 kcal mol^{-1} and possesses an energy barrier of +28.5 kcal mol^{-1} through $TS_{2\rightarrow3}$ (Figure 2).

Amide **4** or its imine tautomer **4′** could then approach **3** to yield complexes **5** or **9**, respectively (Figure 1). Although the binding of the substrates is slightly exothermic in terms of enthalpy (e.g. –1 kcal mol^{-1} for complex **5**), the entropy effect caused by aggregation of molecular species makes the process unfavorable by +23.2 and +43.4 kcal mol^{-1} for the formation of **5** and **9**, respectively, with respect to the reac-

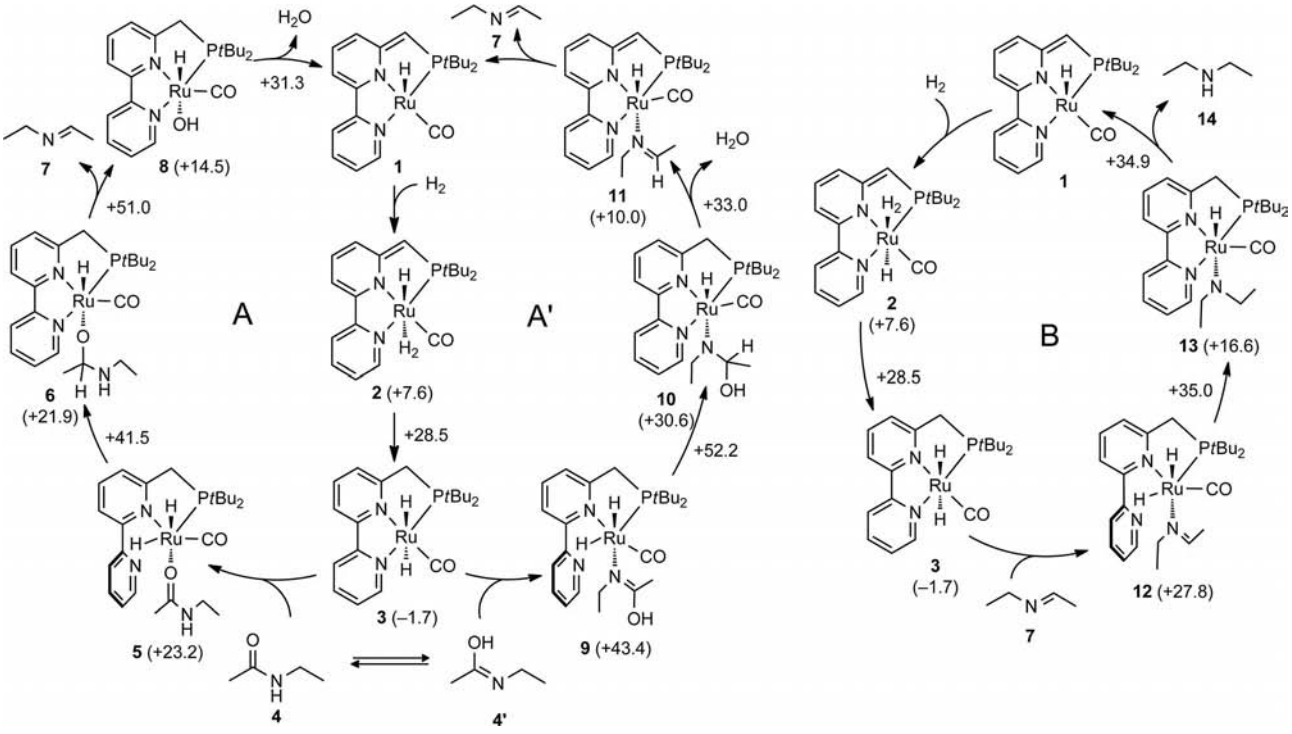

Figure 1. Proposed catalytic cycles for the hydrogenation of amides to secondary amines with C–O cleavage. In catalytic cycle A, imine **7** is released, and it is subsequently hydrogenated in catalytic cycle B. In catalytic cycle A′ addition of H_2 to **11** could give complex **12**, and thus cycles A′ and B could be depicted together. Relative free energies with respect to separate reactants (**1** + **4** + $2H_2$ = 0.0) for all the intermediates (in parentheses) and energy barriers (kcal mol^{-1}) are shown.

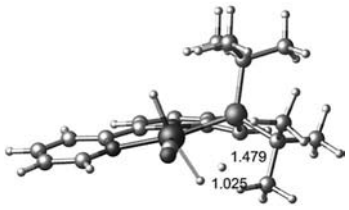

Figure 2. Optimized structure for the transition structure ($TS_{2\rightarrow3}$) corresponding to the aromatization of the pincer complex by reaction of **1** with H_2.

tants (**1** + **4** + H_2). It is also noteworthy that the substrate displaces one of the nitrogen atoms from the ruthenium center at the pincer complex. The lack of coplanarity in the bipyridine framework probably contributes to the unfavorable character of this process. Despite the mentioned endothermicity, no energy barrier has been detected for this ligand exchange.

Compounds **5** and **9** could reduce the carbonyl and imine groups through two possible pathways (Scheme 2). Thus, it could occur by a direct hydride transfer from the ruthenium atom ($TS_{5\rightarrow6}$ and $TS_{9\rightarrow10}$) (Figure 3) or through dearomatization of the pincer complex ($TS_{5\rightarrow6'}$ and $TS_{9\rightarrow10'}$) by hydrogen transfer from the methylene group. The extremely high energy barriers calculated discard dearomatization processes for those reductions, which possess relative energies of +96.7 and +97.3 kcal mol^{-1} for $TS_{5\rightarrow6'}$ and $TS_{9\rightarrow10'}$, respectively. In stark contrast, the barriers for direct hydride transfers are +41.5 kcal mol^{-1} for the amide and +52.2 kcal mol^{-1} for the imine tautomer (Figure 1). The reduction of amide species is likely favored because of the initial stability of the substrates. Although the alternative pathways involving dearomatization of the pincer complex ($TS_{5\rightarrow6'}$ and $TS_{9\rightarrow10'}$) could in principle look unlikely, this kind of six-membered transition structures cannot be ruled out at all, as we shall see later.

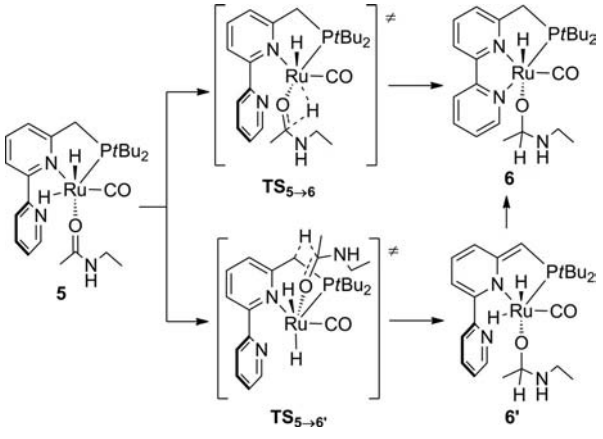

Scheme 2. Alternative pathways for the reduction of double bonds, exemplified by the reduction of intermediate **5**.

The next steps in catalytic cycles A and A′ are clearly divergent. In pathway A, **6** undergoes an internal proton transfer from the amine group to the ruthenium-bonded oxygen, which releases imine **7** and yields the ruthenium–

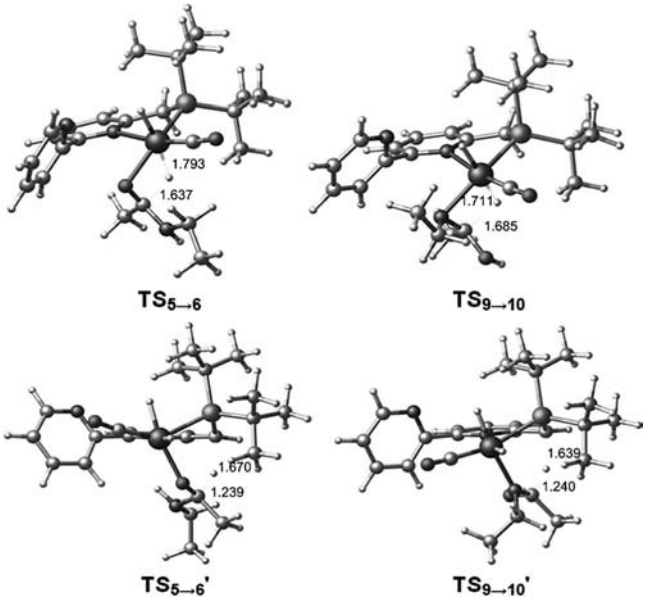

Figure 3. Optimized geometry for the transition states involved in the reduction of amide and imine groups, both through direct proton transfer of one ruthenium hydride ($TS_{5\rightarrow6}$ and $TS_{9\rightarrow10}$) and one proton from the methylene group ($TS_{5\rightarrow6'}$ and $TS_{9\rightarrow10'}$), thus dearomatizing the pincer complex.[19]

hydroxy complex **8** (Figure 1). The transformation is exothermic, but exhibits a relatively high energy barrier of +51.0 kcal mol^{-1}. In the case of **10**, the proton transfer takes place with dearomatization of the pincer complex and releases one water molecule instead of **7**. Interestingly, this transformation has a low barrier (+40.1 kcal mol^{-1}) relative to the above-mentioned dearomatization processes from **5** and **9**. Compound **11** can subsequently release **7** by a simple ligand exchange without energy barrier.[18] The elimination of water in **8** also takes place through a dearomatization process. In this case the energy barrier, +31.3 kcal mol^{-1}, is relatively low, too, and **1** is recovered.

The theoretical calculations on pathways A and A′ reveal similar overall energy barriers (+51.0 and +52.2 kcal mol^{-1}). These somewhat high energy barriers are in agreement with the drastic conditions usually required for reported amide hydrogenations involving C–O cleavage (i.e. 160 °C and 40–100 bar of hydrogen pressure).[5–6] In both catalytic cycles, imine **7** and H_2O are generated as final products, and the main difference, in addition to the initial substrates, is the nature of the rate-determining steps. While in pathway A the key step involves formation of **7**, reduction of the imine group occurs in the case of A′.

Imine **7** must be subsequently hydrogenated, and this happens in catalytic cycle B (Figure 1). The formation of intermediate **3** occurs in the same manner as in A and A′. Then, imine **7** approaches the ruthenium center to form intermediate **12**. As previously described for the formation of **5** and **9**, the approach of the substrate involves the displacement of one of the bipyridine nitrogen atoms. The energetics for this process is also similar, that is, an endergonic transformation due to entropy effects when the aggregate is

formed. The transfer of one ruthenium-bonded hydride over the imine double bond, with an energy barrier of +35.0 kcal mol^{-1}, is a favorable process by 11.2 kcal mol^{-1} (with respect to **12**). It should be noted that the free energies depicted in catalytic cycle B are also referred to the initial reactants (**1** + **4** + 2H_2). In this way, the relative stabilities of the different substrates (**4**, **4′**, and **7**) are also taken into account.

The release of diethylamine (**14**) from intermediate **13** involves dearomatization of the pincer complex. Thus, one methylene hydrogen is transferred to the amine nitrogen. This transformation, which possesses a barrier of +34.9 kcal mol^{-1}, together with the formation of **14**, recovers catalyst **1**. The overall hydrogenation process (**4** + 2H_2 → **14** + H_2O) is thermodynamically favorable by –4.9 kcal mol^{-1}.

The energetics depicted in Figure 1 reveals that both amide **4** and its imine tautomer **4′** can be involved in the hydrogenation process leading to C–O cleavage. The global energy barriers (+51.0 and +52.2 kcal mol^{-1}, respectively) favor the reduction of **4** by only approximately 1 kcal mol^{-1} (catalytic cycles A and A′, Figure 1). The released imine **7** can be more easily hydrogenated in comparison with the initial substrate (cat. cycle B, Figure 1), since the energy barrier is 35.0 kcal mol^{-1}.

As described above, in catalytic cycle A, the approach of **4** to dihydride–ruthenium complex **3** and subsequent hydrogen transfer leads to alkoxide **6**. This intermediate could alternatively evolve as depicted in catalytic cycle C (Figure 4), as proposed by Milstein and co-workers.[7] In this case, the amino group catches one hydrogen atom from the methylene group. The corresponding transition structure $TS1_{6\rightarrow16}$ (Figure 5), with an energy barrier of only +38.1 kcal mol^{-1}, leads to an intermediate ($INT_{6\rightarrow16}$) in which the amide nitrogen is protonated, at a relative energy of 26.3 kcal mol^{-1}.

The pincer complex is dearomatized during this process. Then, ethylamine can easily be released from the carbonyl group through a second transition state ($TS2_{6\rightarrow16}$) (Figure 5), which possesses a relatively low energy barrier of +27.9 kcal mol^{-1}. A second H_2 molecule can rearomatize **16** to give **17**. As **16** is in equilibrium with **1** and acetaldehyde, the barrier for this hydrogenation step must be exactly the same as that for **1** → **3** (28.5 kcal mol^{-1}). It is worth pointing out that the relative energy of $TS_{5\rightarrow6}$ and **6** are different in catalytic cycles A and C. The reason is the different configuration at the chiral center formed during the hydrogenation of the carbonyl group. While in catalytic cycle C the rate-determining step (RDS) is the formation of **6**, with configuration *R*,*R* for the most stable transition state, in catalytic cycle A the RDS involves formation of complex **8**. In this case, the most stable transition structure comes from a substrate (compound **6**) possessing the diastereomeric *R*,*S* configuration (see Supporting Information).

The evolution of **17** is analogous to that of **12** in cycle B. First, one of the ruthenium-bonded hydrides reduces the carbonyl group, which leads to the alkoxide–ruthenium complex **18** with an energy barrier of +33.4 kcal mol^{-1} (Figure 4). During the formation of ethanol (**19**), the pincer complex is again dearomatized through a concerted transition state ($TS_{18\rightarrow1}$) (Figure 5), which results in an energy of only +21.3 kcal mol^{-1}. In this way the catalyst is recovered.

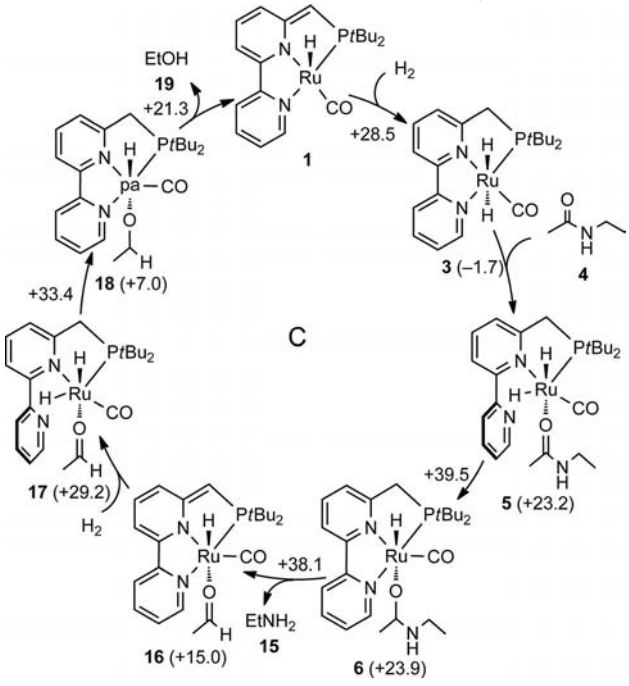

Figure 4. Catalytic cycle for the hydrogenation of amides to primary amines and alcohols with C–N cleavage proposed by Milstein and co-workers. Relative free energies with respect to separate reactants (**1** + **4** + 2H_2 = 0.0) for all the intermediates (in parentheses), and energy barriers (kcal mol^{-1}) are shown. The relative energies of **6** and the previous TS are different from those in catalytic cycle A, because cycles A and C follow different stereoisomeric pathways (see Supporting Information).

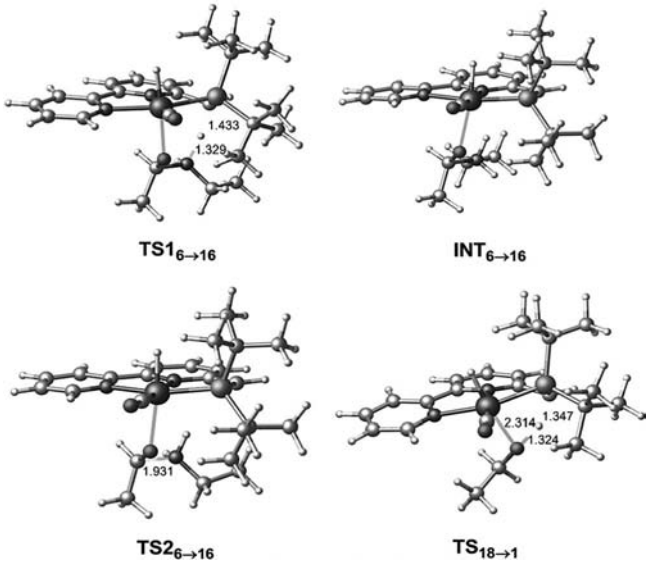

Figure 5. Optimized geometry for the transition structures and intermediate leading to the transformation from **6** to **16** and optimized geometry for $TS_{18\rightarrow1}$. In both processes the pincer complex is dearomatized.

The overall process depicted in catalytic cycle C consists of the hydrogenation of amide **4** with C–N cleavage, so the final products are ethylamine (**15**) and ethanol (**19**). This is an unfavorable transformation, endothermic by 0.8 kcal mol^{-1}. The high, experimentally applied[7] H_2 pressure must increase the concentration of the reactant in the solvent and displace the equilibrium, thus explaining the good conversion achieved.[7]

The key role of the aromatization/dearomatization processes occurring during these transformations is noteworthy. The ease of deprotonation of the methylene group depending on the parent substrate determines the pathway followed by the intermediates. Thus, compounds **5**, **9**, and **12** are unable to dearomatize the pincer complex (the high-energy transition states are collected in the Supporting Information), and the reduction takes place through the transfer of one of the ruthenium-bonded hydrides. On the contrary, the ease with which intermediates **8**, **10**, **13**, and **18** transfer a methylene hydrogen enables the recovery of catalyst **1**. Notably, intermediate **6** can also lead to dearomatization of the pincer complex by the amino group. This feature enables the bifurcation from the classical C–O cleavage to the hydrogenation, in which the C–N bond is dissociated. The relatively low energy barrier for this dearomatization, +38.1 kcal mol^{-1}, which is more than 10 kcal mol^{-1} below that calculated for the catalytic cycle involving C–O bond breaking, accounts for the complete selectivity in this transformation.[7] This lower barrier also explains the relatively mild conditions needed for the hydrogenation to occur with **1** as catalyst, which leads to the alcohol and the primary amine. In this case, the reaction conditions are 10 atm hydrogen pressure and 110 °C in THF,[7] which contrast with the more drastic conditions necessary for C–O cleavage.

The relative energies presented in this work have been calculated at 298 K and 1 atm, and thus they do not correspond to the experimental conditions. In order to assure that the conclusions reported herein are consistent with both the standard conditions and experimental ones, we recalculated the thermodynamic properties of the key transition structures and reactants at 383 K (110 °C) and 10 atm. The results are collected in Table 1. The change in the energy barriers is not significant on increasing temperature and pressure. The aggregation of particles in the transition states (**1** + **4** + H_2) results in a negative activation entropy and consequently in a higher barrier as the temperature increases. However, the effect of the high pressure probably compensates this effect, and the barriers are only increased by 2–4 kcal mol^{-1}.

Table 1. Relative energies for the key transition structures involved in catalytic cycles A, A′, and C at the standard conditions and the experimental conditions employed by Milstein.[7]

	$\Delta G^{\neq}$ (kcal mol^{-1})	
	298 K, 1 atm	383 K, 10 atm
$TS_{6\rightarrow 8}$	+51.0	+54.1
$TS_{9\rightarrow 10}$	+52.2	+56.9
$TS_{5\rightarrow 6}$	+39.5	+42.7

Conclusion

The hydrogenation of amide groups has been assessed by means of DFT calculations by using the M06 approach. The classical C–O cleavage and the newly reported C–N bond breaking[7] have been compared by using the bipyridyl-based Ru^{II} pincer complex **1** as catalyst in our calculations.

In the mechanism for the reduction in which the C–O bond is cleaved to yield the secondary amine, the participation of both amide **4** and its imine tautomer **4′** has been considered. The similar energetics involved in the reduction of these compounds (+51.0 and +52.2 kcal mol^{-1} for amide and imine, respectively) reveals that both isomers could be appropriate substrates for the formation of secondary amines with C–O cleavage. The high energy barriers are in good agreement with the drastic conditions usually employed in the transformation (i.e. high hydrogen pressures and temperatures above 160 °C).

Once the carbonyl group is reduced in catalytic cycle A, intermediate **6** can be transformed into **7** + **8** in the key step of the overall process. However, **6** can also evolve by a stepwise process. First, one of the methylene hydrogen atoms is transferred to the amine group, which leads to a new intermediate in which the pincer complex is dearomatized. The subsequent fast release of the protonated amine from the carbonyl group results in the C–N bond breaking reported by Milstein. This stepwise process has an energy barrier of +38.1 kcal mol^{-1}, thereby explaining the complete selectivity provided by catalyst **1** for C–N bond cleavage. This energetics equally accounts for the much milder conditions required by this reaction (10 atm H_2 pressure, 110 °C in THF)[7] in comparison with that described for the hydrogenation yielding the secondary amine.

The aromatization/dearomatization of the pincer complex, depending on the intermediate, plays the leading role in the above-mentioned selectivity and guides the transformation to the products obtained experimentally.

Supporting Information (see footnote on the first page of this article): Stereoisomeric pathway descriptions, images of transition state structures, Cartesian coordinates, energies, and imaginary frequencies (transition states) for all the calculated stationary points.

Acknowledgments

The Spanish Ministry of Education and Science (CTQ2010-18938/BQU), FEDER, and the Junta de Extremadura (PRI08-A032) have supported this investigation financially. D. C. thanks the Spanish Ministerio de Educación y Ciencia for a fellowship and the Research, Technological Innovation and Supercomputing Center of Extremadura (CénitS) for supporting the use of LUSITANIA computer resources. Special thanks go to Pedro Cintas, José L. Jiménez, and David Milstein for helpful comments on the manuscript.

[1] P. M. Rylander, *Hydrogenation Methods*, Academic Press, London, **1985**, and references therein.
[2] J. Seyden-Penne, *Reductions by the Alumino and Borohydrides in Organic Synthesis*, 2nd ed., Wiley-VCH, New York, **1997**.
[3] B. Wojcik, H. Adkins, *J. Am. Chem. Soc.* **1934**, *56*, 2419–2424.
[4] G. Beamson, A. J. Papworth, C. Philipps, A. M. Smith, R. Whyman, *J. Catal.* **2010**, *269*, 93–102.
[5] C. Hirosawa, N. Wakasa, T. Fuchikami, *Tetrahedron Lett.* **1996**, *37*, 6749–6752.
[6] A. A. Núñez Magro, G. R. Eastham, D. J. Cole-Hamilton, *Chem. Commun.* **2007**, 3154–3156.
[7] E. Balaraman, B. Gnanaprakasam, L. J. W. Shimon, D. Milstein, *J. Am. Chem. Soc.* **2010**, *132*, 16756–16758.
[8] J.-W. Handgraaf, E. J. Meijer, *J. Am. Chem. Soc.* **2007**, *129*, 3099–3103.
[9] a) D. T. Tommaso, S. A. French, A. Zanotti-Gerosa, F. Hancock, E. J. Palin, C. R. A. Catlow, *Inorg. Chem.* **2008**, *47*, 2674–2687; b) M. Lei, W. Zhang, Y. Chen, Y. Tang, *Organometallics* **2010**, *29*, 543–548; c) J.-W. Handgraaf, J. N. H. Reek, E. J. Meijer, *Organometallics* **2003**, *22*, 3150–3157; d) C. Hedberg, K. Källström, P. I. Arvidsson, P. Brandt, P. G. Andersson, *J. Am. Chem. Soc.* **2005**, *127*, 15083–15090; e) D. A. Alonso, P. Brandt, S. J. M. Nordin, P. G. Andersson, *J. Am. Chem. Soc.* **1999**, *121*, 9580–9588.
[10] T. Privalov, J. S. M. Samec, J.-E. Bäckvall, *Organometallics* **2007**, *26*, 2840–2848.
[11] N. Blaquiere, S. Diallo-Garcia, S. I. Gorelsky, D. A. Black, K. Fagnou, *J. Am. Chem. Soc.* **2008**, *130*, 14034–14035.
[12] M. J. Frisch, G. W. Trucks, H. B. Schlegel, G. E. Scuseria, M. A. Robb, J. R. Cheeseman, G. Scalmani, V. Barone, B. Mennucci, G. A. Petersson, H. Nakatsuji, M. Caricato, X. Li, H. P. Hratchian, A. F. Izmaylov, J. Bloino, G. Zheng, J. L. Sonnenberg, M. Hada, M. Ehara, K. Toyota, R. Fukuda, J. Hasegawa, M. Ishida, T. Nakajima, Y. Honda, O. Kitao, H. Nakai, T. Vreven, J. A. Montgomery Jr., J. E. Peralta, F. Ogliaro, M. Bearpark, J. J. Heyd, E. Brothers, K. N. Kudin, V. N. Staroverov, R. Kobayashi, J. Normand, K. Raghavachari, A. Rendell, J. C. Burant, S. S. Iyengar, J. Tomasi, M. Cossi, N. Rega, J. M. Millam, M. Klene, J. E. Knox, J. B. Cross, V. Bakken, C. Adamo, J. Jaramillo, R. Gomperts, R. E. Stratmann, O. Yazyev, A. J. Austin, R. Cammi, C. Pomelli, J. W. Ochterski, R. L. Martin, K. Morokuma, V. G. Zakrzewski, G. A. Voth, P. Salvador, J. J. Dannenberg, S. Dapprich, A. D. Daniels, Ö. Farkas, J. B. Foresman, J. V. Ortiz, J. Cioslowski, D. J. Fox, *Gaussian 09*, Revision A.1, Gaussian, Inc., Wallingford CT, **2009**.
[13] Y. Zhao, D. G. Truhlar, *Theor. Chem. Acc.* **2008**, *120*, 215–241.
[14] Y. Zhao, D. G. Truhlar, *Acc. Chem. Res.* **2008**, *41*, 157–167.
[15] D. Andrae, U. Häusserman, M. Dolg, H. Stoll, H. Preuss, *Theor. Chim. Acta* **1990**, *77*, 123–141.
[16] A. W. Ehlers, M. Böhme, D. Dapprich, A. Gobbi, A. Hölwarth, V. Jonas, K. F. Köhler, R. Stegmann, A. Veldkamp, G. Frenking, *Chem. Phys. Lett.* **1993**, *208*, 111–114.
[17] A. V. Marenich, C. J. Cramer, D. G. Truhlar, *J. Phys. Chem. B* **2009**, *113*, 6378–6396.
[18] The release of **7** from **11** may not be necessary. In catalytic cycle A′ addition of H_2 to **11** can give complex **12**, and thus cycles A′ and B would be depicted together.
[19] The figures were prepared with CYLView: C. Y. Legault, CYLView, 1.0b, Universite de Sherbrooke, Quebec, **2009**, http://www.cylview.org.

Received: April 27, 2011
Published Online: May 24, 2011

